1.5-µm Indium Phosphide-based Quantum Dot Lasers and Optical Amplifiers

Sven Bauer (1), Vitalii Sichkovskyi (1), Ori Eyal (2), Tali Septon (3), Annette Becker (1), Igor Khanonkin, Gadi Eisenstein (2), and Johann Peter Reithmaier (1), (*)

(1) Institute of Nanostructure Technologies and Analytics, CINSaT, University of Kassel, Kassel, 34132, Germany.
(2) Department of Electrical Engineering and the Russel Berry Nanotechnology Institute, Technion, Haifa, 3200, Israel.
(3) Nvidia Mellanox, Yokneam, 2069200, Israel.
(*) jpreith@ina.uni-kassel.de

Abstract: An overview will be given on the progress of quantum dot laser materials addressing the telecom C band and their high potential for the application in optical communication systems, where temperature stability of the device performance as well as a narrow linewidth emission plays an important role. Device results of quantum dot lasers and optical amplifiers will be shown, and the physical background discussed.

1. Introduction

In nanomaterials, the electronic properties can be strongly modified by geometrical dimensions, if one can scale down the objects to the nanometer scale. There was already an early prediction of improved laser performance in threshold current density and temperature stability using quantum dots [1, 2]. Quantum dot materials based on self-organized strain-driven formation of nano-islands during the epitaxial growth process allow the fabrication of practically defect-free nanomaterials. This technique can be applied for different material combinations as long as there is a large enough lattice mismatch between them. This so-called Stranski-Krastanow growth mode [3] was first successfully applied for lasers in the InAs on GaAs material system [4] and later transferred to InAs on InGaAlAs [5]. However, due to the much-reduced strain in this material combination, the favorite formation geometry is an elongated island, which are called quantum dashes. They are more wire-like than dot-like with some advantages and disadvantages. To get atom-like discrete energy levels, dot-like QDs are favorized. This was made possible by some modifications in the growth technique [6], which allow the suppression of surface diffusion and an acceleration of the nucleation process. A drawback of the Stranski-Krastanow growth technique is the statistical size fluctuation, which results in broadening of the gain spectrum and a possible overlap between ground and excited optical transitions. A strong improvement could be obtained by a much better control of the nucleation process by optimizing the surface roughness of the nucleation layer. With that, a strong reduction of the inhomogeneous linewidth broadening was obtained [7]. In figure 1, an atomic force microscope (AFM) picture is shown for a quantum dot layer consisting of InAs QDs grown on AlGaInAs lattice matched to InP.

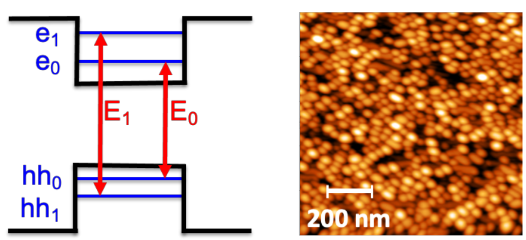

Figure 1. On the left: Simplified term scheme for a quantum dot with ground state transition E_0 and excited state transition E_1. On the right: AFM picture on nearly circular InAs QDs grown on AlGaInAs surface with a dot density in the order of about 5 x 10^{10} cm^{-2}.

2. Laser material growth and Device fabrication

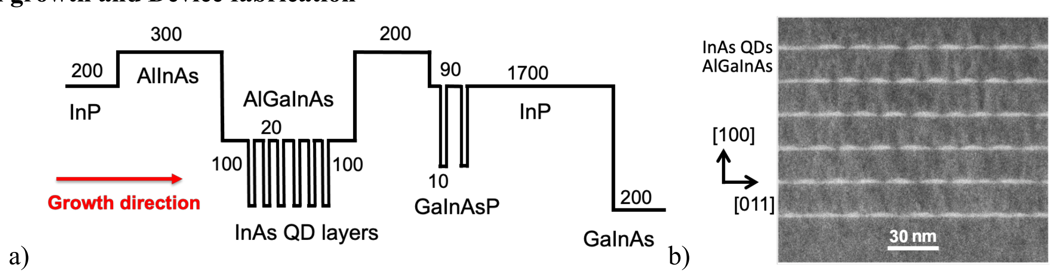

Figure 2. (a) Schematic conduction band diagram for the layer structure of a high-speed QD laser. The additional GaInAsP layers are needed as etch stop layers for grating fabrication in DFB lasers [8]. (b) HAADF-STEM image of the cross-section of the active region of such a laser with 6 QDLs [9].

The QD layers with high dot densities and low size fluctuation are embedded in a separate confinement heterostructure (SCH) with AlInAs waveguide layers (see figure 2a). The top cladding layer consists of InP and includes additional etch stop layers for grating definition of laterally defined distributed feedback (DFB) lasers fabrication. The active region of the laser materials used for device fabrication and for which the results are shown in this paper, is undoped. A cross section transmission electron microscope (TEM) image is shown in figure 2b.

From this epi-wafers, ridge waveguide lasers and SOAs were fabricated by optical lithography and dry/wet chemical etching. For DFB lasers, a lateral grating is defined by electron beam lithography. For short cavity lasers, the back facets were high reflection (HR) coated, while for SOAs both facets were anti reflection (AR) coated.

3. Static laser properties

The lasers were fabricated with different cavity lengths between 230 up to about 1 mm. In figure 3, the laser characteristics in continuous wave (CW) (see figure 3a) and in pulsed mode (figure 3b) are shown as a function of the heat-sink temperature. From the pulsed mode operation, the characteristic temperatures are evaluated and plotted in figure 3c. Record values of T_0 = 144 K (till 80°C) and T_1 of > 900 K (till 110°C) are obtained [10]. These values are much higher one can usually obtain with conventional quantum well lasers [11].

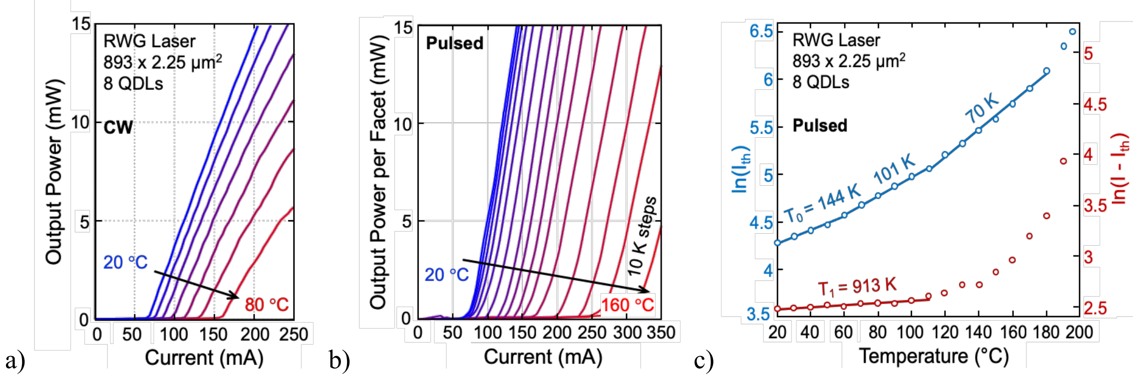

Figure 3. *(a) Light output characteristics of a QD RWG laser with 8 QDLs, 893 µm cavity length and a ridge width of 2.25 µm in CW, (b) pulsed operation and (c) evaluated characteristic temperatures T_0 and T_1 [10].*

4. Dynamic laser properties

Short devices with HR coated back facets were mounted on a high frequency submount with a partially adapted impedance matching contacts. The small signal modulation characteristics are shown in Figure 4a at different bias currents at 20 °C. The inset show the bandwidth at different heat-sink temperatures. Although the bandwidth is reduced with temperature, a digital modulation up to 26 GBit/s at 80°C is still possible, as shown in Figure 4b.

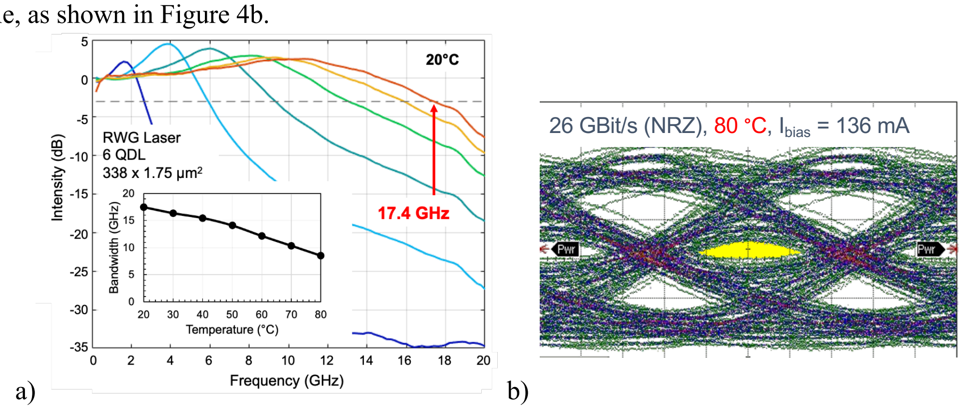

Figure 4. *(a) Small signal response of a 338 µm long RWG QD laser for different bias currents (30, 40, 60, 90, 120 and 160 mA). The inset shows the temperature dependence of the maximum obtainable modulation bandwidth. (b) Large signal response (NRZ modulation) at 80 °C with a data rate 26 GBit/s [10].*

5. Spectral properties of QD DFB lasers

The linewidth of conventional semiconductor DFB lasers is mainly limited by the linewidth enhancement factor (LEF) of the material, which is typically in the order of 3-5 resulting for a linewidth broadening by more than an order of magnitude in comparison to the theoretical limit. In QD materials, which exhibit a narrow ground state gain and neglectable contributions from higher order transitions, a very symmetric optical gain function can be obtained. This results in a low LEF in the order of < 1 and consequently the linewidth should go towards the theoretical limits. In figure 5, the device characteristics of a QD DFB laser are shown. With such a device, a high side mode suppression (SMSR) of more than 50 dB and a single wavelength output power near to 60 mW can be obtained (see figure 5a). And indeed, record values in the linewidth of about 30 kHz could be obtained (see figure 5b), which is more than an order of magnitude lower than for pure monolithic quantum well DFB lasers, without an external cavity approach [13].

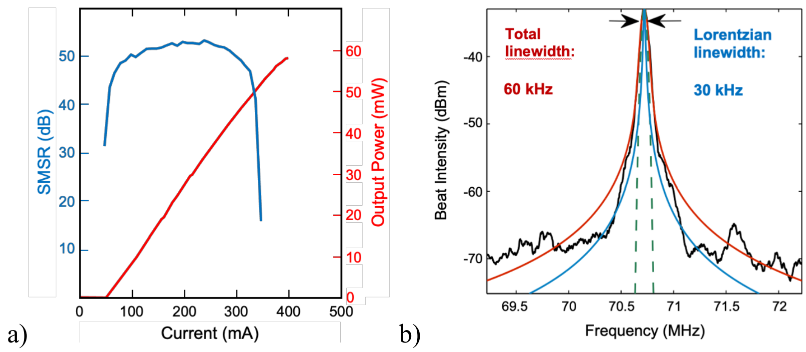

Figure 5. (a) *Laser characteristics of a QD DFB-Laser (side mode suppression ratio SMSR in blue, light output characteristic in red) [12]. (b) Emission line of the same laser measured by optical frequency comb interferometry. The data are fitted by a Voigt profile (red) and the corresponding Gaussian (dashed line) and Lorentzian (blue) profiles are shown separately [13].*

6. High temperature operating QD SOAs

For the integration of III-V optoelectronic components into a Si-based photonic platform, in particular, the temperature control is difficult or impossible. For this purpose, not only integrated lasers but also other elements such as optical amplifiers should exhibit a low temperature sensitivity. As shown above, QD materials are less temperature sensitive than quantum well counterparts. Also, semiconductor optical QD amplifiers (QD-SOA) show excellent high-temperature operation. In Figure 6, the amplified signals of a 28 GBit/s data stream are shown at 45°C and 96°C, respectively, without any signal deterioration.

Figure 6*. Amplification of a 28 Gbit/s signal by an QD SOA at 1590 nm at temperatures of (a) 45°C and (b) 96°C [14].*

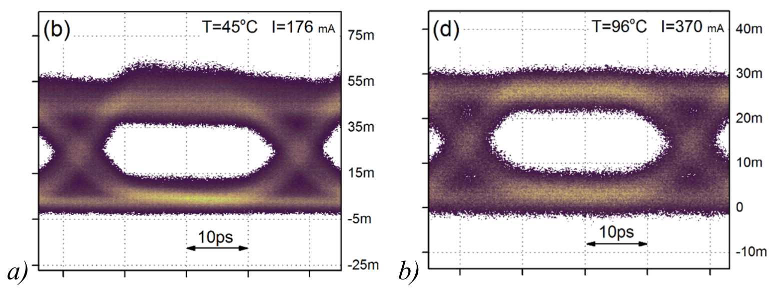

7. Conclusions and Acknowledgements

The QD material now also available for the telecom C band wavelength range, exhibits significantly improved temperature stability for lasers and SOAs in comparison to conventional quantum well gain materials due to the intrinsic atom-like material properties. With this type of material also the linewidth limitation originated by the energy dispersion properties in quantum well or bulk like media can be overcome by QD materials and the linewidth broadening phenomena suppressed by more than one order of magnitude. Together with the much-reduced back reflection sensitivity of QD lasers [15], QD materials are very promising as best choice for III-V on Si integration platforms in the 1.3 µm [16] and 1.55 µm [17] wavelength range.

We would like to acknowledge funding by the European Commission (projects SEQUOIA, Moicana) and the national BMBF (projects Monolop and PEARLs). This work was also partially funded by the Israeli Science Foundation, grant number 460/21.

References

[1] Y. Arakawa et al. Appl. Phys. Lett., vol. 40, no. 11, p. 939, 1982. doi: 10.1063/1.92959.
[2] M. Asada et al., IEEE J. Quantum Electron., vol. 22, no. 9, p. 1915, 1986. doi: 10.1109/JQE.1986.1073149.
[3] I. N. Stranski et al Monatshefte für Chemie. Band 71, Nr. 1, Dezember 1937, ISSN 0026-9247, S. 351–364, doi:10.1007/BF01798103
[4] N. Kirstaedter et al., Electron. Lett., vol. 30, no. 17, p. 1416, 1994. doi: 10.1049/el:19940939.
[5] R. Schwertberger et al., IEEE Photon. Technol. Lett., vol. 14, no. 6, pp. 735–737, 2002. doi: 10.1109/ LPT.2002.1003076.
[6] C. Gilfert et al., Appl. Phys. Lett. 96, no. 19, p. 191,903, 2010. doi: 10.1063/1.3428956.
[7] S. Banyoudeh et al., J. Cryst. Growth, vol. 425, pp. 299, 2015. doi: 10.1016/j. jcrysgro.2015.03.027.
[8] S. Banyoudeh et al., IEEE Photon. Technol. Lett, vol. 28, no. 21, p. 2451, 2016. doi: 10.1109/LPT.2016.2600508.
[9] W. Rudno-Rudzinski et al., Physica Stat. Sol. A, vol. 215, no. 4, p. 1,700,455, 2018. doi: 10.1002/pssa.201700455.
[10] A. Abdollahinia et al., Optics Express, vol. 26, no. 5, p. 6056, 2018. doi: 10.1364/OE.26.006056.
[11] B. Witzigmann et al., IEEE J. Sel. Topics Quantum Electron., vol. 9, no. 3, p. 807, 2003. doi: 10.1109/JSTQE.2003.818859.
[12] A. Becker et al., Appl. Phys. Lett., vol. 110, no. 18, p. 181,103, 2017. doi: 10.1063/1.4982716
[13] T. Septon et al., Optica, vol. 6, no. 8, pp. 1071–1077, 2019. doi: 10.1364/OPTICA.6.001071.
[14] O. Eyal et al., Optics Express, vol. 25, no. 22, pp. 27,262–27,269, 2017. doi: 10.1364/OE.25.027262.
[15] J. Duan et al., IEEE Photonics Tech. Lett. **31**, 345–348 (2019). doi: 10.1109/lpt.2019.2895049.
[16] Z. Zhang et al., IEEE J. Sel. Top. Quantum Electron 25, 1–9 (2019). doi: 10.1109/JSTQE.2019.2916884.
[17] S. Bauer et al., IEEE Nanotechnology Magazine, 23 (April 2021). doi: 10.1109/MNANO.2020.3048103 (invited paper)